Catalysis Today 182 (2012) 54–59

Contents lists available at SciVerse ScienceDirect

Catalysis Today

journal homepage: www.elsevier.com/locate/cattod

In situ study of oxidation states and structure of 4 nm CoPt bimetallic nanoparticles during CO oxidation using X-ray spectroscopies in comparison with reaction turnover frequency

Fan Zheng[a,c,1], Selim Alayoglu[b,c,1], Vladimir V. Pushkarev[b,c], Simon K. Beaumont[b,c], Colin Specht[a,c], Funda Aksoy[d], Zhi Liu[d], Jinghua Guo[d], Gabor A. Somorjai[a,c,*]

[a] Materials Sciences Division, Lawrence Berkeley National Lab, Berkeley, CA, United States
[b] Chemical Sciences Division, Lawrence Berkeley National Lab, Berkeley, CA, United States
[c] University of California Berkeley, Department of Chemistry, Berkeley, CA, United States
[d] Advanced Light Source, Lawrence Berkeley National Lab, Berkeley, CA, United States

ARTICLE INFO

Article history:
Received 3 July 2011
Received in revised form 5 October 2011
Accepted 11 October 2011
Available online 14 December 2011

Keywords:
In situ X-ray absorption spectroscopy
Ambient pressure X-ray photo-electron spectroscopy
Bimetallic nanoparticles
CoPt alloys
Oxidation states
Cycling pressure
CO oxidation
Turnover frequency

ABSTRACT

In situ near edge X-ray absorption fine structure (NEXAFS) spectroscopy and ambient pressure X-ray photoelectron spectroscopy (AP-XPS) were performed to monitor the oxidation state and structure of 4 nm CoPt nanoparticles during the reaction of CO with O_2 – a model oxidation reaction. In addition, reversible changes in the oxidation state of cobalt as a function of cycling CO and O_2 pressure (in the range of millitorr to 60 Torr) were quantified and compared. Turnover frequency reaction data was also obtained for the CoPt nanoparticles and correlated with the oxidation states and structures observed spectroscopically. These findings indicate that separated from the effect of partial pressure of the reactant gases, chemical state and structure changes of the CoPt nanoparticles during CO oxidation are important factors in determining the rate of the reaction.

© 2011 Elsevier B.V. All rights reserved.

1. Introduction

Cobalt is well known for its use in the catalytic hydrogenation reactions of CO and CO_2 to produce gaseous or liquid hydrocarbons, with a long history of producing synthetic fuels. Here we consider its role in the model oxidation reaction of CO to CO_2. By choosing to explore model reactions and carefully characterizing the catalyst under reaction conditions it is hoped that we can gain a greater understanding of the fundamental factors that determine catalyst behavior. A significant number of previous studies have been conducted on CO oxidation of Co oxide or Co–Pt bimetallics [1–9]. In these studies it has been suggested that the oxidation state of Co plays a critical role in the catalytic reaction mechanism: specifically, cobalt oxide provides oxygen to combine with the adsorbed CO molecules and Co is itself then re-oxidized to provide a new active site.

Bimetallic CoPt nanoparticles have recently drawn attention in many areas of catalysis in a quest to reduce precious metal content while maintaining optimum catalytic reactivity. Stamenkovic et al. [10] have documented a family of Pt and 3d transition metal alloy catalysts that are more effective in oxidizing CO than monometallic Pt. Likewise, bimetallic CoPt nanoparticle catalysts have recently found application in reforming small sugar molecules in water [11]. CO oxidation is a model reaction that has been studied extensively by us and others. The goal of our present work is therefore to understand the role of oxidation state and elemental composition changes of one such typical bimetallic catalyst's surface reactivity. To achieve this, we embarked on a combined catalytic and in situ spectroscopic study of bimetallic 4 nm CoPt nanoparticles used as catalysts for CO oxidation in the 10 mTorr–100 Torr pressure range and at 125 °C.

We previously [12] studied the evolution of the cobalt oxidation state under reducing and oxidizing conditions for 4 nm Co and CoPt nanoparticles. We found that the presence of platinum

* Corresponding author at: UC-Berkeley, Department of Chemistry, D56 Hildebrand Hall, Berkeley, CA, United States. Tel.: +1 510 642 4053.
E-mail address: somorjai@berkeley.edu (G.A. Somorjai).
[1] These authors contributed equally to this work.

0920-5861/$ – see front matter © 2011 Elsevier B.V. All rights reserved.
doi:10.1016/j.cattod.2011.10.009

facilitates the rapid reduction of cobalt oxides in H_2 at low temperature (38 °C) – the reduction happens much more easily than occurs for pure Co. In addition, reversible changes of the oxidation state of cobalt in the nanoparticles as a function of reactant pressure (in the range of millitorr to 36 Torr) were quantified and compared. Using in situ X-ray spectroscopies we report on exploring a real catalytic reaction – CO oxidation with 4 nm CoPt nanoparticles, as a function of reaction pressure. These spectroscopic results are then correlated to turnover frequency measurements under an identical range of conditions.

2. Experimental

2.1. Materials

$Pt(acac)_2$, $Co(acac)_2$, polyvinylpyrollidone (PVP, $M_w \sim 55{,}000$), benzyl alcohol and 1,6 hexanediol were purchased from Aldrich. Ethylene glycol, acetone, ethanol (absolute) were purchased from VWR. All chemicals were used as received.

4 nm CoPt alloy catalyst was synthesized according to a methodology which was recently reported [12]. Briefly, $Pt(acac)_2$ (acac = acetylacetonate) and $Co(acac)_2$ precursors were co-nucleated in ethylene glycol in the presence of PVP as a capping agent in an oil bath at 240 °C (Fig. 1). Pure Co nanoparticles were prepared by reduction of $Co(acac)_2$ in benzyl alcohol in the presence of PVP by 1,6-hexanediol at 150 °C. The individual, as prepared nanoparticles were seen to be truly bimetallic each comprising Pt and Co as demonstrated by STEM/EDS analysis in Fig. 1c and also reported elsewhere [12]. Colloidal nanoparticles of CoPt were characterized using TEM (Jeol 2100-LaB_6, and FEI CM300) and STEM/EDS (Jeol 2100-FE). Langmuir–Blodgett (LB) films of these nanoparticle samples on Au (for AP-XPS and NEXAFS) or Si (for catalytic measurements) substrates were prepared using a LB trough (Nima Technology, M611). Two-dimensional LB films were examined with scanning electron microscopy (Zeiss Ultra55). Since the Pt-catalyzed decomposition temperature for PVP is beyond 300 °C, [13] although it will remain present throughout the reaction it will not decompose allowing gases to diffuse through it and not blocking the active sites with carbonaceous decomposition products.

AP-XPS studies were carried out at beamline 9.3.2 in the Advanced Light Source, Berkeley, California. Pt 4f, Au 4f (substrate), core levels were monitored in vacuum or controlled gas atmospheres in the sub-torr pressure range and at temperatures between 25 °C and 125 °C. XPS depth profiles were obtained using 250 eV, 350 eV and 630 eV incident photon energies corresponding to mean free paths of 4 Å, 6 Å and 11 Å, respectively for Pt 4f and Au 4f photo-electrons. XP spectra were recorded until no further spectral changes could be observed in the continuous scans, which took about 10 min under 100 mTorr H_2 and about 30 min under the CO/O_2 reaction conditions at 125 °C. To compare with X-ray absorption spectroscopy experiments, a total pressure of 80 mTorr and 800 mTorr with O_2:CO = 1.4:1 were used during AP-XPS measurements.

The in situ soft X-ray absorption measurements were conducted at beamline 7.0.1 in the Advanced Light Source with a similar methodology to those described in the previous study on reduction/oxidation on the CoPt nanoparticles [12]. The cobalt oxidation state was monitored with NEXAFS spectroscopy by using the compensation current to the sample (the flow of electrons replacing those emitted from the sample) to determine the total electron yield signal. This permits the recording of spectra in the presence of reactive gases under the conditions used for CO oxidation. The cell was described in detail previously, but briefly it comprises a reaction chamber in which the 2D sample is placed separated from ultra high vacuum by a 100 nm thick Si_3N_4 window and supplied with gas via a manifold of Parker mass flow controllers to control gas composition. A valve between the reactor and a vacuum line is used to control the overall pressure as monitored using baratron gauges at both the inlet and outlet to the reactor. X-ray absorption at the Co L-edges was recorded with 0.3 eV resolution. The oxidation state of cobalt was obtained by least squares fitting to a series of reference spectra as described previously (see supporting information) [12]. Repeat Co L-edge absorption spectra were recorded at the same spot as well as different spots and no X-ray induced artifacts were observed. As noted in our previous study [12], care must be taken in recording the spectra to ensure that the system has arrived at a stable state after changing the pressure of reactant gases. Accordingly, at each pressure point a series of spectra were taken (over a time scale of 20–50 min) at the Co L-edge until no further changes between spectra were observed. This indicates the Co has arrived at a stable or meta-stable state or is only changing very slowly on the timescale of the reaction.

Turnover frequency (TOF) catalytic measurements for the CO oxidation reaction were carried out using a pressure-variable batch reactor operating in the 10 mTorr–100 Torr pressure range. Reaction gases were first admitted to a mixing chamber using a gas manifold while closely monitoring the pressure of individual reactants. The gas mixtures were then introduced to the reaction chamber before beginning the reaction by heating the sample to a set temperature point of 125 °C. The reaction was monitored by flowing a small quantity of the reaction mixture through a leak valve to the analysis chamber (typically held at $\sim 10^{-9}$ Torr), which was equipped with a quadruple mass spectrometer (Stanford Research Systems RGA200). To avoid diffusion limitations at low pressures (<1 Torr), the reaction mixture in the batch reactor was constantly stirred using a motor-driven fan. The number of surface Pt sites on the 2D nanoparticle samples was determined using the rate of ethylene hydrogenation, a method previously adopted by our group owing the structure insensitive nature of this reaction. This was performed using a flow reactor and calculations based on the reported TOF of 11.8 ethylene molecules per surface Pt site per second under our conditions (20 °C, 10 Torr ethylene and 100 Torr H_2). For the ethylene/H_2 reaction using 10 Torr ethylene and 100 Torr H_2, activation energy between 20 °C and 70 °C was found to be 7.0 kcal mol^{-1}, and was in good agreement with literature values [14]. The geometric area of the nanoparticles was also calculated using the TEM-projected average particle size, SEM-projected coverage of the nanoparticles in fractions of a monolayer (submonolayer on silicon layer), the geometric area of Si substrate, and the surface packing density of the metals, and was within a 20% error window of the surface area derived from the ethylene/H_2 reaction (see Fig. S3 for detailed information). TOFs for the CO/O_2 reaction were calculated under steady-state conversion regimes corresponding to both chemically (i.e. NEXAFS) and structurally (i.e. AP-XPS) stable (or meta-stable) states of the catalyst. The agreement between TEM, SEM and ethylene hydrogenation rates indicates it is appropriate for small molecules such as CO, O_2 and CO_2, which can diffuse through the capping like ethylene, not to pretreat the catalyst, as to do so may alter the nanoparticles or impair activity through the formation of carbonaceous material [15]. The samples for both catalysis and X-ray spectroscopies are therefore studied as made/supported without prior treatments to attempt removal of the capping agent.

3. Results and discussion

Employing X-ray spectroscopies allows exploration of the catalysts' real structures under reaction conditions – in particular we have adopted two synchrotron based methodologies to achieve this

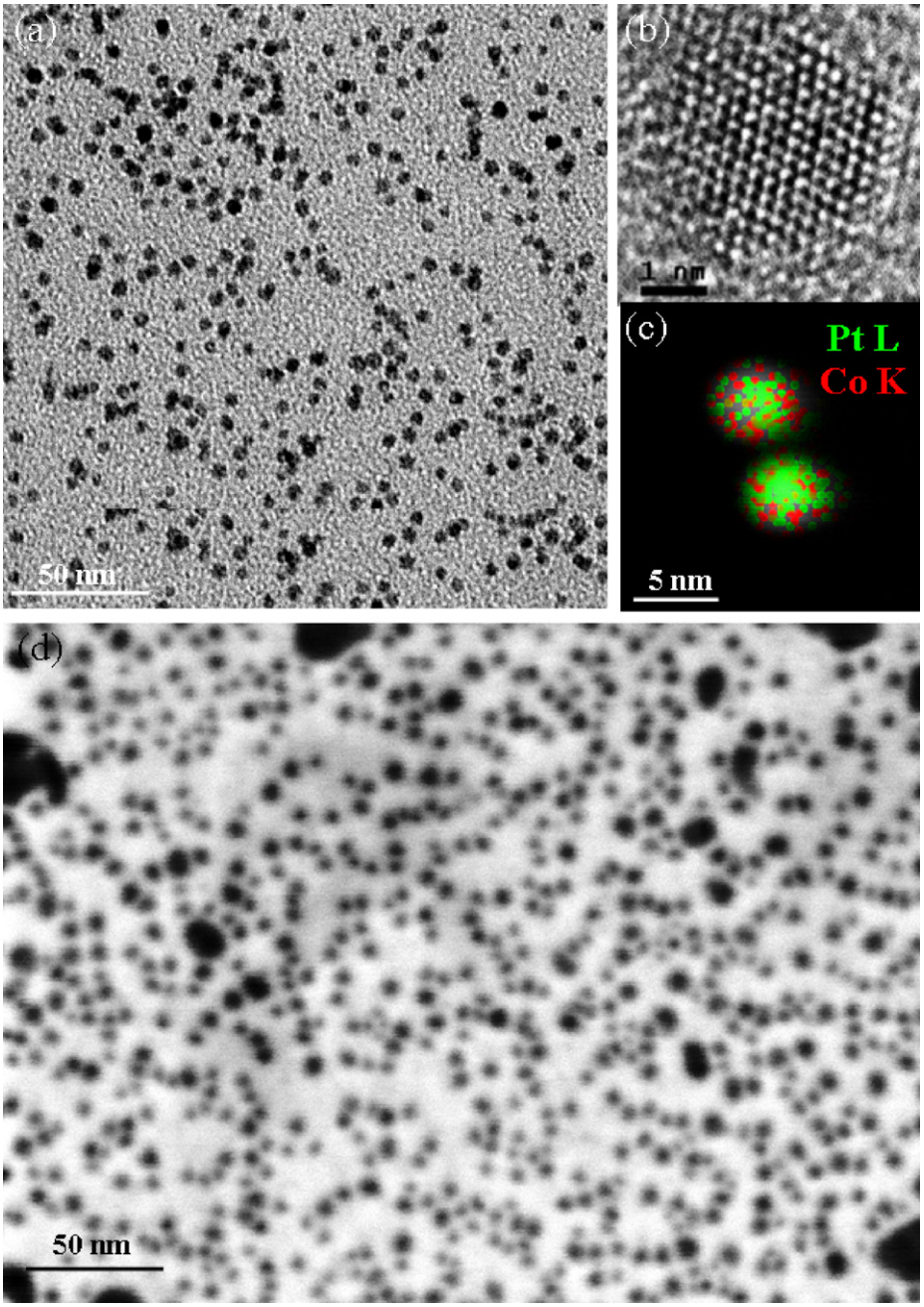

Fig. 1. (a) TEM and (b) HRTEM images of the as-synthesized CoPt nanoparticles. (c) Representative STEM/EDS elemental mapping of Pt L (green) and Co K (red) edges. (d) SEM image of the Langmuir–Blodget film of CoPt nanoparticles after the CO/O_2 reaction studies. (For interpretation of the references to color in this figure legend, the reader is referred to the web version of the article.)

goal: firstly Near Edge X-ray Absorption Fine Structure (NEXAFS) spectroscopy and secondly Ambient Pressure X-ray Photoelectron Spectroscopy (AP-XPS). Fig. 2 shows a sequence of NEXAFS spectra acquired for the 4 nm CoPt alloy catalyst under the cycling pressures of reactant gases. As described previously [12], this is made possible because rather than following emitted electrons directly, we use the fact these electrons (which in the presence of gas are quickly absorbed and thus cannot themselves be measured easily) must be offset by electrons from ground potential, and so a "compensation current" can be measured to obtain a total electron yield signal. The key differences in the spectra on changing the reactant gas pressure can be seen in the presence or absence of shoulders appearing 1–2 eV above the pure metallic cobalt resonance at ~779 eV – note that the CoPt particle is initially fully reduced while the subsequent dosing of O_2 and CO was monitored by the continuous scan of NEXAFS spectra until no change on the spectra happened. This should eliminate the pre-reducing effect on the oxidation state of Co.

A more quantitative picture of the evolution of the cobalt's oxidation state under reaction conditions is given by the results of least squares component fitting to a number of reference spectra as described previously [12] (see supporting information).

The results are given in Fig. 3, which shows the changes in the % of cobalt for CoPt alloy catalyst in each of the three different possible oxidation states as the reactant (O_2 and CO) pressure is increased from a few millitorr to 60 Torr then decreased back to a few millitorr. Here the increasing and decreasing of reactant pressures share the same *x*-axis to better demonstrate the hysteresis process and

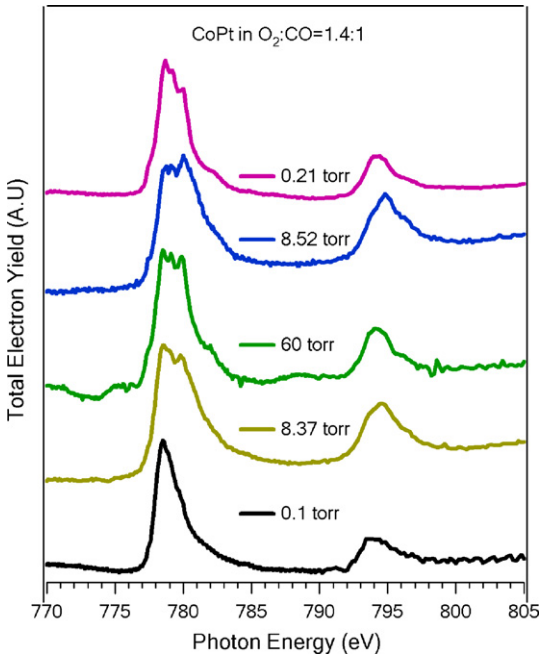

Fig. 2. Examples of Co L-edge absorption spectra obtained at different O_2 and CO partial pressure conditions for 4 nm CoPt nanoparticle samples. In this study the total pressure of O_2, CO and He was varied with a fixed ratio of O_2:CO:He = 1.4:1:28 at 125 °C. Pressures shown in the figure are the total pressure of O_2 and CO cycling from low to high (starting from bottom) and back to low in a range of several millitorr to 60 Torr reactant pressure ($P_{CO} + P_{O_2}$).

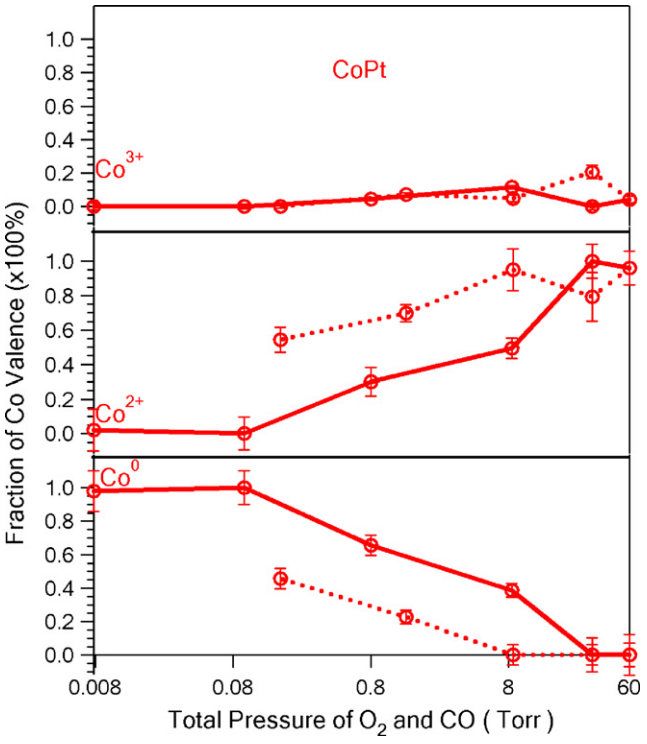

Fig. 3. The fraction of Co in each of its three oxidation states during exposure of the 4 nm CoPt alloy catalyst to the reactant gases, as determined by least squares fitting of the NEXAFS spectra to known reference data (see supporting information). The experiment was conducted with a reactant gas mixture of O_2:CO:He = 1.4:1:28 at 125 °C. Reactant (O_2 and CO) pressure increases was cycled from a few millitorr to 60 Torr and then back to low pressure. The Co^{2+} data represents the sum of components fitted to two different coordination types (O_h and T_d). (See supporting materials S2 for further details). Error bars are calculated through the error propagation from residue sum of squares of difference between the spectrum and the fit, ignoring the systematic errors. Solid line represents the pressure goes upward and dotted line represents the pressure goes downward. *X*-axis indicates the total pressure of O_2 and CO.

this is different from the previous oxidation and reduction study [12], where the increase and decrease of pressure were separately indicated in the *x*-axis. The ratio of all gases was kept constant: The reactant gas ratio O_2:CO:He (balance) was kept constant at 1.4:1:28 throughout the experiment. Prior to CO oxidation both nanoparticle samples were treated in 1 atm H_2 at 125 °C. Under reaction conditions a significant exchange of Co^0 (initially 100% and 80% for CoPt and Co, respectively) to Co^{2+} states occurs as the reactant pressure is increased. Near the maximum pressure, some cobalt is seen to be fully oxidized to Co^{3+} for CoPt samples, both from the least squares fits and from a shoulder at 780.5 eV on the spectra shown in Fig. 2. For comparison we also made measurements on pure Co nanoparticles at the same condition for comparison (see supporting materials S2). The major result is that at high pressure of O_2 and CO cobalt's oxidation state tends to be similar between pure Co and CoPt alloy nanoparticles. This is expected since it is in the O_2 rich reaction condition.

As mentioned above we previously reported on the ability of platinum when incorporated into these particles to change the susceptibility to oxidation and ease of reduction [12]. The behavior observed under actual reaction conditions is broadly similar to that seen previously: as the pressure is decreased again Co^{3+} disappears and the fraction of Co^{2+} also returns partially towards its original state, although some hysteresis is observed. The incomplete reversal in the state of the cobalt as the overall reaction pressure is lowered again could originate in a number of underlying reasons. For Pd it has been reported that such effects are caused by O_2 diffusion [16], however for the present case the favorable formation of bulk cobalt oxide is the most likely candidate. It was shown that [4] CO tends to block O_2 adsorption less on the pre-oxidized Co than on the pre-reduced Co. Since more O_2 is adsorbed when cobalt is already oxidized, once the pressure decreases from the maximum Co in the CoPt alloy nanoparticles remains in a more oxidized state than at the same partial pressure while the pressure is rising.

To understand this more fully a second question arises – what is the structure of the two metals within the particle? This issue is addressed by the second type of X-ray spectroscopy – ambient pressure XPS, which, by using a tunable X-ray source, allows us to probe the structure at different depths within the nanoparticles. This is achieved by varying the kinetic energy of the emitted electrons and thus the depth within the sample from which they can originate and still escape the material. By bringing a differentially pumped cone very close to the sample [17] it is again possible to record spectra under near ambient conditions (up to ~1 Torr).

This method was therefore used to study the metal composition on the surface and in the subsurface regions of the 4 nm CoPt alloy nanoparticles during CO oxidation. In particular we were able to follow the Pt 4f signal at 71 eV (normalized to the underlying Au [4f, 84 eV]) as a function of probing depth and gas pressure (Fig. 4). The relative composition at different depths inside the approximately spherical nanoparticles can then be estimated by recourse to their known particle size of 4 nm from TEM and their known bulk composition from single particle EDS analysis (Pt:Co 55:45). Incident photon energies were selected as a trade off of incident photon flux at beamline 9.3.2 and the broadest range of possible escape depths; energies of 250 eV, 350 eV and 630 eV were selected. This corresponds to electrons with a mean free path of 4 Å, 6 Å and 11 Å – thus sensitive to different depths within the 2 nm radius particles. (It must be remembered there are relatively very few atoms at the core of a particle owing the small fraction of overall volume at the center of the sphere.) In the vacuum case, conventional laboratory XPS (an Al Kα source, 1486 eV incident photons) was also used and the result obtained when probing 2 nm to the very center of the

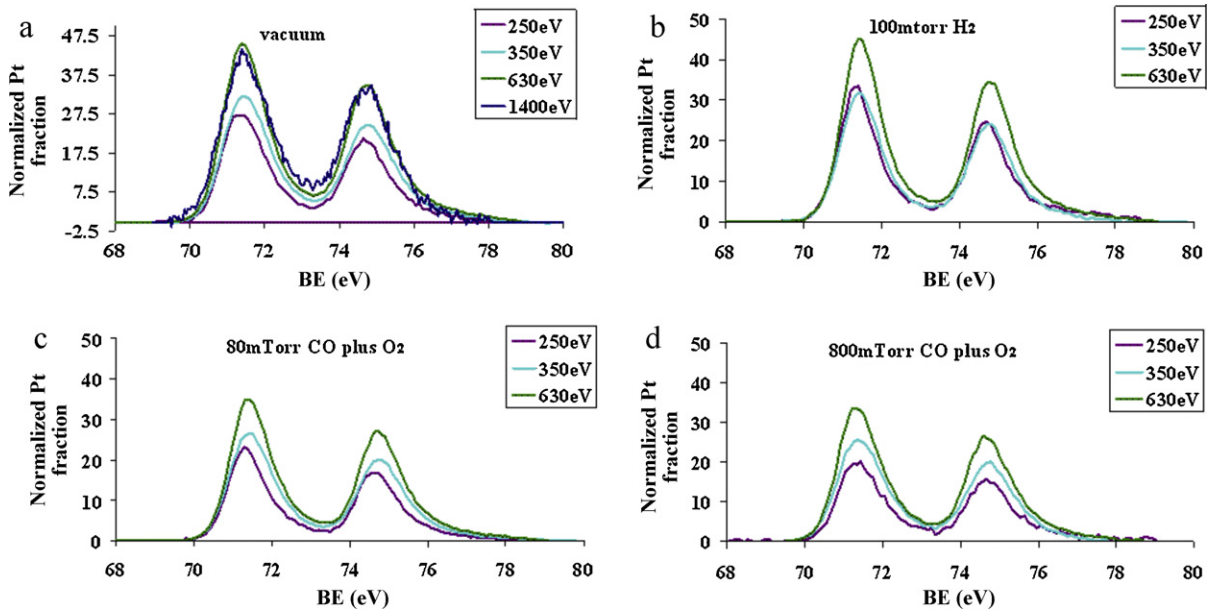

Fig. 4. Normalized XP spectra of CoPt alloy nanoparticles taken using different photoelectron energies under various temperature and pressure conditions: (a) vacuum, 25 °C; (b) 100 mTorr H_2, 125 °C; (c) 80 mTorr total CO + O_2, 125 °C; (d) 800 mTorr total CO + O_2, 125 °C. *y*-Axis shows the normalized Pt 4f signal and *x*-axis the binding energy. Each figure shows XP spectra corresponding to photon energies of 250 eV, 350 eV, 630 eV (AP-XPS) and, in addition, 1400 eV (lab XPS with Al Kα) taken only at vacuum (a).

nanoparticles is in good agreement with that calculated from our synchrotron XPS model.

A typical set of spectra is shown in Fig. 5a. From these spectra a crude model can be derived for illustrative purposes, as described in more detail in the supporting information section, to estimate the ratio of Pt to Co in each shell or layer – the normalized Pt fraction at each escape depth is shown in Fig. 5b and the corresponding appearance of a cross section of a 1/8th spherical cone through the nanoparticle is shown in Fig. 5c.

The key result is that from under vacuum to being reduced in H_2 at 125 °C it is clear there is a significant surface segregation of Pt to the surface – this is even apparent from the spectra shown in Fig. 5a in which the purple and blue spectra correspond to roughly 42% and 63% of the atoms present respectively and yet differ only fractionally in intensity. In contrast under reaction conditions of CO and O_2 there is a significant exchange of Co to the surface region, as seen from the decrease in intensity of the surface Pt (that probed with 250 eV photons). The implication is Co being pulled out from the core of the atom – a reasonable observation given the respective adsorption energies of O_2 on the two metals (100 kcal mol^{-1} for Co versus 67 kcal mol^{-1} for Pt, CO adsorbs equally preferably on Co or Pt [18]). It is also notable that the oxidation state of the Co (obtained from NEXAFS above) changes as the surface fraction of Co increases, from almost all metallic at 80 mTorr (even though some cobalt has already reached the surface layers), to ~30% oxidized at 800 mTorr once more cobalt is in the near surface region – this is also indicated in the model schematics in Fig. 5.

Having carefully characterized the system under a series of typical reaction conditions it is instructive to now compare these results to those obtained for the oxidation of CO to CO_2 in catalytic runs

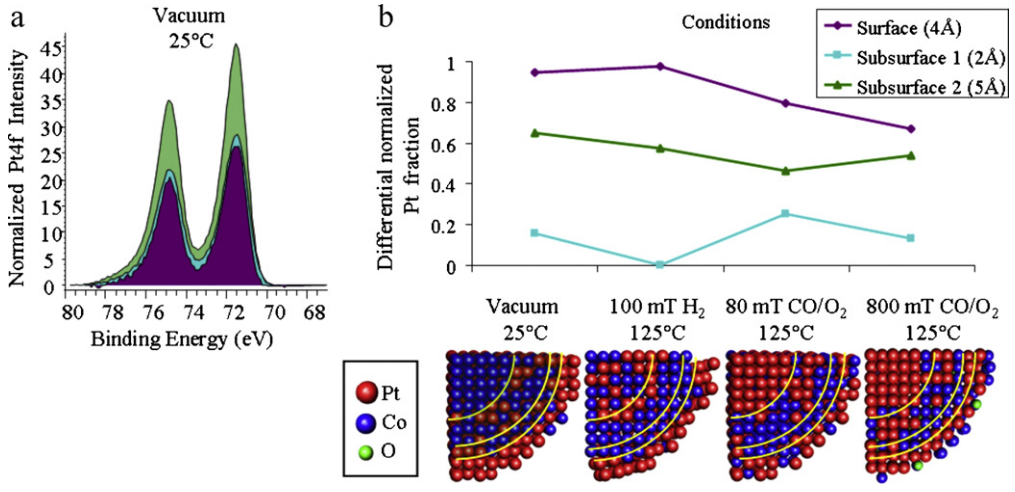

Fig. 5. (a) Ambient pressure Pt 4f XP spectra of 4 nm CoPt alloy nanoparticles under vacuum and at 25 °C at photoelectron energies of 250 eV, 350 eV and 630 eV. (b) Normalized atomic fraction of Pt corresponding to probing depths of around 4 Å, 6 Å and 11 Å as shown by the color coded regions of the XP spectra in (a). (c) Cartoons show the 2D cross-sections of the 1/8th spherical cone of the 3D model clusters constructed with the atomic fraction of Pt present in each region. Red balls represent Pt, blue balls Co and green balls O. Yellow guide lines enclose the regions most sensitively probed by each photon energy: 0–4 Å, 4–6 Å, and 6–11 Å. (For interpretation of the references to color in this figure legend, the reader is referred to the web version of the article.)

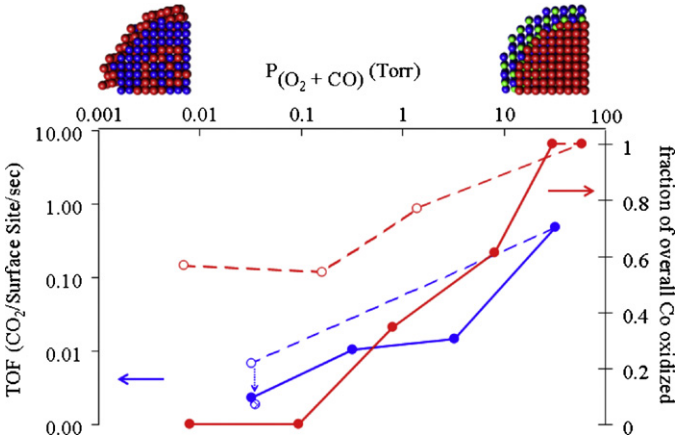

Fig. 6. Plots of turnover frequencies in CO_2/surface site/sec (blue) and oxidized fraction of Co as determined by NEXAFS spectroscopy (red) as a function of O_2 and CO pressures in torr. An O_2:CO ratios of 1.4:1 was used for both turnover rate and NEXAFS spectroscopy studies. Solid spheres and lines show the data acquired while increasing reactant pressure and hollow spheres and dashed lines show the return direction while decreasing reactant pressure. The "⊗" symbol highlights the TOF measurement obtained at 43 mTorr O_2 and CO pressure following re-reduction in H_2 (20 Torr/250 °C) after the reaction cycle. Atom cluster models show the approximate arrangement of Pt (red), Co (blue) and O (green) atoms derived from spectroscopic measurements as above for the high and low extremes of pressure presented. (For interpretation of the references to color in this figure legend, the reader is referred to the web version of the article.)

– these were performed in a batch reactor and monitored using a quadruple mass spectrometer at various pressures of reactant gases in a similar range to those explored spectroscopically – again the reaction rate was observed as the overall reactant pressure (O_2:CO still 1.4:1) was increased from a few millitorr to 43 Torr, then decreased back to a few millitorr. The turnover frequencies obtained are presented in Fig. 6, along with the fraction of the cobalt which was oxidized (Co^{2+} and Co^{3+}) from the NEXAFS spectroscopy data above. The solid lines show the rate increasing with increasing reactant pressure. The dotted lines show the rate of reaction as the pressure is lowered back to a few millitorr and a marked hysteresis is observed – both in the catalysis and the spectroscopy. This is important because it is otherwise hard to isolate an effect due to nanoparticle structure from the effect of the partial pressure of reactants on the overall rate. At 25 mTorr O_2, 18 mTorr CO the reaction rate is seen to be four times greater after exposure to the higher reactant pressure than before. From the NEXAFS spectroscopy results the cobalt is still more oxidized under these conditions and the AP-XPS results indicate it is very likely that Co remains near the surface under these conditions (as it is when exposed to the reactive gases at higher pressures), whereas the surface is predominantly Pt under these conditions after reduction in H_2. The origin of this effect being the reactant induced changes in the material is further re-enforced by the fact that re-reduction of the samples in H_2 to complete the cycle (shown as "⊗") returns the catalytic activity to its initial lower value.

4. Conclusions

To summarize in situ X-ray spectroscopy measurements and catalytic turnover frequency measurements were performed on 4 nm CoPt alloy nanoparticles and the fractions of Co oxidation states mapped while cycling the total pressure of O_2, CO and He between a few millitorr and one bar total pressure. Ambient pressure XPS indicates a significant change in the elemental distribution within each bimetallic particle, changing from Pt covered surfaces under reducing conditions to a significant surface presence of Co in the case of the reacting catalyst in CO and O_2. Turnover frequency measurements were then correlated with these results and a hysteresis observed in cycling between oxidizing and reducing conditions, indicating the importance of oxidation state of Co, particle structure induced by the reaction conditions as well as just the reactant partial pressures in contributing to the overall CO oxidation rate for these bimetallic nanoparticles.

Acknowledgements

This work was supported by the Director, Office of Energy Research, Office of Basic Energy Sciences of the U.S. Department of Energy under Contract DE-AC02-05CH11231. The Advanced Light Source is supported by the Director, Office of Science, Office of Basic Energy Sciences, of the U.S. Department of Energy under Contract No. DE-AC02-05CH11231. The authors also acknowledge support of the National Center for Electron Microscopy, Lawrence Berkeley Lab, which is supported by the U.S. Department of Energy under Contract # DE-AC02-05CH11231. Work at the Molecular Foundry was supported by the Director, Office of Science, Office of Basic Energy Sciences, Division of Material Sciences and Engineering, of the U.S. Department of Energy under Contract # DE-AC02-05CH11231.

Appendix A. Supplementary data

Supplementary data associated with this article can be found, in the online version, at doi:10.1016/j.cattod.2011.10.009.

References

[1] L. Guczi, T. Hoffer, Z. Zsoldos, S. Zyade, G. Maire, F. Garin, Journal of Physical Chemistry 95 (1991) 802–808.
[2] Y.J. Mergler, A. vanAalst, J. vanDelft, B.E. Nieuwenhuys, Applied Catalysis B: Environmental 10 (1996) 245–261.
[3] A. Torncrona, M. Skoglundh, P. Thormahlen, E. Fridell, E. Jobson, Applied Catalysis B: Environmental 14 (1997) 131–145.
[4] P. Thormahlen, M. Skoglundh, E. Fridell, B. Andersson, Journal of Catalysis 188 (1999) 300–310.
[5] J. Jansson, Journal of Catalysis 194 (2000) 55–60.
[6] P. Broqvist, I. Panas, H. Persson, Journal of Catalysis 210 (2002) 198–206.
[7] J. Jansson, A.E.C. Palmqvist, E. Fridell, M. Skoglundh, L. Osterlund, P. Thormahlen, V. Langer, Journal of Catalysis 211 (2002) 387–397.
[8] M.J. Pollard, B.A. Weinstock, T.E. Bitterwolf, P.R. Griffiths, A.P. Newbery, J.B. Paine, Journal of Catalysis 254 (2008) 218–225.
[9] W.L. Yim, T. Kluner, Journal of Physical Chemistry C 114 (2010) 7141–7152.
[10] V.R. Stamenkovic, B.S. Mun, M. Arenz, K.J.J. Mayrhofer, C.A. Lucas, G.F. Wang, P.N. Ross, N.M. Markovic, Nature Materials 6 (3) (2007) 241–247.
[11] R.R. Davda, J.W. Shabaker, G.W. Huber, R.D. Cortright, J.A. Dumesic, Applied Catalysis B: Environmental 56 (1–2) (2005) 171–186.
[12] F. Zheng, S. Alayoglu, J.H. Guo, V. Pushkarev, Y.M. Li, P.A. Glans, J.L. Chen, G. Somorjai, Nano Letters 11 (2011) 847–853.
[13] Y. Borodko, S.E. Habas, M. Koebel, P.D. Yang, H. Frei, G.A. Somorjai, Journal of Physical Chemistry B 110 (2006) 23052–23059.
[14] J.N. Kuhn, C.K. Tsung, W. Huang, G.A. Somorjai, Journal of Catalysis 265 (2009) 209–215.
[15] Y. Borodko, S.M. Humphrey, T.D. Tilley, H. Frei, G.A. Somorjai, Journal of Physical Chemistry C 111 (2007) 6288–6295.
[16] S. Ladas, R. Imbihl, G. Ertl, Surface Science 219 (1989) 88–106.
[17] D.F. Ogletree, H. Bluhm, G. Lebedev, C.S. Fadley, Z. Hussain, M. Salmeron, Review of Scientific Instruments 73 (2002) 3872–3877.
[18] I. Toyoshima, G.A. Somorjai, Catalysis Reviews: Science and Engineering 19 (1979) 105–159.